

Fifth-order susceptibility unveils growth of thermodynamic amorphous order in glass-formers

S. Albert¹, Th. Bauer^{2,†}, M. Michl², G. Biroli^{3,4}, J.-P. Bouchaud⁵,
 A. Loidl², P. Lunkenheimer², R. Tourbot¹,
 C. Wiertel-Gasquet¹, F. Ladieu^{1*}

¹SPEC, CEA, CNRS, Université Paris-Saclay,

CEA Saclay Bat 772, 91191 Gif-sur-Yvette Cedex, France,

²Experimental Physics V, Center for Electronic Correlations and Magnetism,
 University of Augsburg, 86159 Augsburg, Germany,

[†] Present address: Institute for Machine Tools and Industrial Management,
 Technical University of Munich, 85748 Garching, Germany,

³IPhT, CEA, CNRS, Université Paris-Saclay,

CEA Saclay Bat 774, 91191 Gif-sur-Yvette Cedex, France,

⁴LPS, Ecole Normale Supérieure, 24 rue Lhomond, 75231 Paris Cedex 05, France,

⁵Capital Fund Management, 23 rue de l'Université, 75007 Paris, France

*Corresponding author: francois.ladieu@cea.fr.

Glasses are ubiquitous in daily life and technology. However the microscopic mechanisms generating this state of matter remain subject to debate: Glasses are considered either as merely hyper-viscous liquids or as resulting from a genuine thermodynamic phase transition towards a rigid state. We show that third and fifth order susceptibilities provide a definite answer to this longstanding controversy. Performing the corresponding high-precision nonlinear dielectric experiments for supercooled glycerol and propylene carbonate, we find strong support for theories based upon thermodynamic amorphous order. Moreover, when lowering temperature, we find that the growing transient domains are compact – that is their fractal dimension $d_f = 3$. The glass transition may thus represent a class of critical phenomena different from canonical second-order phase transitions for which $d_f < 3$.

The glassy state of matter, despite its omnipresence in nature and technology (1), continues to be one of the most puzzling riddles in condensed-matter physics (1, 2): For all practical purposes, glasses are rigid like crystals but they lack any long-range order. Some theories describe glasses as kinetically constrained liquids (3), becoming so viscous below the glass transition that they seem effectively rigid. By contrast, other theories (4, 5) are built on the existence of an underlying thermodynamic phase transition to a state where the molecules are frozen in well defined, yet disordered positions. This so-called "amorphous order" cannot be revealed by canonical static correlation functions, but rather by new kinds of correlations [i.e. point-to-set correlations or other measures of local order (6, 7)] that have now been detected in recent numerical simulations (7–9). In these theories, thermodynamic correlations lock together the fluctuations and response of the molecules, which collectively rearrange over some length-scale ℓ , ultimately leading to rigidity. In this thermodynamic scenario, ℓ is proportional to a power of $\ln(\tau_\alpha/\tau_0)$ where τ_α is the structural relaxation time and τ_0 is the microscopic time-scale, generally smaller than

1ps (4, 5). Because equilibrium measurements require a time larger than τ_α , they cannot be performed in the range where ℓ is very large since this would require exponentially long times. This limitation is essentially why the true nature of glasses is still a matter of intense debate.

Here, we propose a pioneering strategy to unveil the existence of a thermodynamic length ℓ that grows upon cooling. Instead of only varying the temperature T , we also vary the non-linear order k of the response of supercooled liquids. This is motivated by a general, although rarely considered (10), property of critical points: At a second order critical temperature T_c , the linear susceptibility χ_1 associated to the order parameter is not the only diverging response. As a function of temperature, all the higher order responses χ_{2m+1} with $m \geq 1$ diverge even faster than χ_1 itself. This comes from the fact that the divergencies of all the χ_{2m+1} have the same origin, namely the divergence of the length ℓ . By using the appropriate scaling theory, it can be shown that the larger m , the stronger the divergence in temperature. As theoretically shown below, transposing this idea to glasses requires taking into account that the putative “amorphous” or hidden order in supercooled liquids (7, 11) is not reflected in χ_1 itself, but only in higher-order response functions χ_{2m+1} with $m \geq 1$. This idea is indeed supported by previous measurements and analyses of the third order susceptibility χ_3 (12–16). We report results on the fifth order susceptibility $\chi_5(T)$ and compare them to $\chi_3(T)$ in two canonical glass forming liquids, glycerol and propylene carbonate. If critical phenomena really play a key role for the glass transition, χ_5 should increase much faster than χ_3 as the liquid becomes more viscous.

This scenario can be understood by means of a theoretical argument based on previous work (17) and further detailed in (18). Suppose that $N_{\text{corr}} = (\ell/a)^{d_f}$ molecules are amorphously ordered over the length-scale ℓ , where a is the molecular size and d_f is the fractal dimension of the ordered clusters. This implies that their dipoles, oriented in apparently random positions, are essentially locked together during a time τ_α . We expect that in the presence of an external electric field E oscillating at frequency $\omega \geq \tau_\alpha^{-1}$, the dipolar degrees of freedom of these molecules contribute to the polarisation per unit volume as

$$p = \mu_{\text{dip}} \frac{\sqrt{(\ell/a)^{d_f}}}{(\ell/a)^d} F \left(\frac{\mu_{\text{dip}} E \sqrt{(\ell/a)^{d_f}}}{kT} \right) \quad (1)$$

where μ_{dip} is an elementary dipole moment, F is a scaling function such that $F(-x) = -F(x)$, and $d = 3$ the dimension of space. This states that randomly locked dipoles have an overall moment $\sim \sqrt{N_{\text{corr}}}$, and that we should compare the energy of this “super-dipole” in a field to the thermal energy. Equation 1 is motivated by general arguments involving multi-point correlation functions through which d_f can be given a precise meaning (18) and is fully justified when ℓ diverges, in particular in the vicinity of a critical point such as the Mode-Coupling transition or the spin-glass transition. In the latter case, Eq. 1 is in fact equivalent to the scaling arguments of (19), provided one performs the suitable mapping between the magnetic formalism of (19) and ours.

Expanding Eq. 1 in powers of E , we find the “glassy” contribution to p :

$$\begin{aligned} \frac{p}{\mu_{\text{dip}}} &= F'(0) \left(\frac{\ell}{a} \right)^{d_f-d} \left(\frac{\mu_{\text{dip}} E}{kT} \right) + \frac{1}{3!} F^{(3)}(0) \left(\frac{\ell}{a} \right)^{2d_f-d} \left(\frac{\mu_{\text{dip}} E}{kT} \right)^3 + \\ &+ \frac{1}{5!} F^{(5)}(0) \left(\frac{\ell}{a} \right)^{3d_f-d} \left(\frac{\mu_{\text{dip}} E}{kT} \right)^5 + \dots \end{aligned} \quad (2)$$

Because d_f must be less or equal to d , we find that the first term, contributing to the usual linear dielectric constant $\chi_1(\omega)$, cannot grow as ℓ increases. This simple theoretical argument explains why we do not expect spatial glassy correlations to show up in $\chi_1(\omega)$. The second term, contributing to the third-order dielectric constant, does grow with ℓ provided $d_f > d/2$. Although $d_f < d$ close to a standard second order critical point (20) such as the spin-glass transition, several theories suggest (4, 5, 21, 22) that ordered domains are compact ($d_f = d$), in which case $(\frac{\ell}{a})^{2d_f-d} = (\frac{\ell}{a})^d = N_{\text{corr}}$, as assumed in our previous papers (17, 23). The third term of Eq. 2 reveals that the fifth-order susceptibility $\chi_5(\omega)$ should diverge as ℓ^{3d_f-d} . Therefore, the joint measurement of $\chi_3(\omega)$ and $\chi_5(\omega)$

provides a direct way to estimate d_f experimentally, through the following relation:

$$|\chi_5| \propto |\chi_3|^{\mu(d_f)}; \quad \mu(d_f) = \frac{3d_f - d}{2d_f - d}; \quad d_f(\mu) = d \frac{\mu - 1}{2\mu - 3} \quad (3)$$

where the exponent $\mu(d_f)$ is equal to 2 when the dynamically correlated regions are compact ($d_f = d$), and is higher otherwise. We predict two key results that can be obtained from χ_5 and χ_3 susceptibility measurements. First, if amorphous order increases approaching the transition, the frequency dependence should be more anomalous [i.e. more humped (18)] for $\chi_5(\omega)$ than for $\chi_3(\omega)$. Second, the growth of χ_5 should be much stronger than that of χ_3 when lowering the temperature, following $\chi_5 \sim \chi_3^2$ if we assume compact amorphous domains. Our work provides experimental evidence that these predictions indeed hold and suggests that the glass transition represents a new type of critical phenomenon with growing length and time scales but with $d_f = d$, in contrast to the spin-glass transition that instead displays (19) canonical critical behavior with $d_f \approx 2.35$.

We measured $\chi_5(\omega)$ in two canonical glass formers, glycerol and propylene carbonate, by applying a field of amplitude E and of frequency $f = \omega/(2\pi)$, see (18). The fifth-order response is $\propto \chi_5 E^5$, and orders of magnitude smaller than the cubic and linear ones, given by $\propto \chi_3 E^3$ and $\propto \chi_1 E$ respectively. We avoided any contributions of χ_3 and of χ_1 by measuring the signal at 5ω , which only contains the component $\chi_5^{(5)}$ of the fifth order susceptibility (18). We measured $\chi_5^{(5)}$ with two independent setups due to the very small amplitude, optimized along complementary strategies. One setup (in Augsburg) was designed to achieve the highest possible field (reaching 78 MV/m). We optimized sensitivity with a differential technique using two samples of different thicknesses in the other setup (Saclay, see Fig. S1 of (18)), which required lower fields (up to 26 MV/m).

We have obtained the values of $|\chi_5^{(5)}(\omega)|$ for glycerol at various frequencies and temperatures by using the two aforementioned techniques (Fig. 1A). A clear peak arises for a given T in $|\chi_5^{(5)}(\omega)|$ for a frequency $f_{\text{peak}} \simeq 0.22f_\alpha$ where the α -relaxation frequency f_α , defined by the peak of the out-of-phase linear susceptibility, is indicated by arrows in Fig. 1A. Even though the data were determined by two independent setups, the overall agreement is remarkable (Fig. 1B). The most accurate comparison is possible at 204K where f_{peak} is well inside the frequency range accessible by the two setups. The two spectra at 204K coincide on the low frequency side of the peak (18). On the other side of the peak, a discrepancy between the two sets of data progressively increases with frequency, reaching a constant factor of 4 at the highest frequencies (Fig. 1B). Apart from the value of the electric field, the main difference between the two experiments is the number of applied field cycles n . The Saclay setup measured the stationary responses ($n \rightarrow \infty$), whereas n remained finite in the Augsburg setup [similarly to (24)], ranging from $n = 2$ at the lowest frequencies to $n \propto f$ at the highest frequencies. The two setups give the same results for $\chi_5^{(5)}$ because at sufficiently low values of f/f_α , the response of the supercooled liquid is likely to instantaneously follow the field. By contrast, at higher frequencies $\omega \geq \tau_\alpha^{-1}$ the finite cycle number may play a role, making a quantitative treatment of this effect difficult (18). Our further analysis relies on the behavior of the peaks of $\chi_5^{(5)}$, and more precisely on their relative evolution with temperature, which reasonably agrees in the two setups (see below).

The qualitative features of $|\chi_5^{(5)}(\omega)|$ (Fig. 1A-B) are reminiscent of those of the third harmonic cubic susceptibility $|\chi_3^{(3)}(\omega)|$, (12, 13). Both quantities exhibit a humped shape, with a peak located at the same frequency $f_{\text{peak}} \approx 0.22f_\alpha$, as well as a strong increase of the height of the peak as the temperature is decreased. These two distinctive features are important since they are specific signatures of glassy dynamical correlations (17), in contrast to trivial systems without correlations (25). In this case, the modulus of all higher-order non linear susceptibilities monotonously decreases with frequency (18, 25).

To quantitatively compare the frequency dependency of the susceptibilities $\chi_k^{(k)}$ of order k , we plotted $|\chi_k^{(k)}(f/f_\alpha)/\chi_k^{(k)}(0)|$ of glycerol for $k = 5, 3$, and 1 ($\chi_1^{(1)}$ is the linear susceptibility noted χ_1 above) (Fig. 1C). The peak amplitude for $k = 5$ is strongly enhanced compared to $k = 3$ – that is the higher the nonlinear order k , the more anomalous the frequency dependence (Fig. 1C and Figs. S2-S3 of (18)). This behavior is a decisive result and fully consistent with our scaling analysis. For archetypical glass formers, we can always fit the linear susceptibility by assuming a sum of Debye relaxations where $\chi_{1, \text{Debye}} \propto 1/(1 - i\omega\tau)$. We do this by choosing

a suitable distribution $\mathcal{G}(\tau)$ of relaxation times τ (26) caused by dynamical heterogeneities. Because the trivial response discussed above also obeys $\chi_{1,\text{trivial}} \propto 1/(1 - i\omega\tau)$, we have used (18, 25) the same distribution $\mathcal{G}(\tau)$ to calculate the trivial responses $\chi_{k,\text{trivial}}^{(k)}$ for $k = 3$ and 5. For a given $k > 1$, a large difference exists between the experimental spectrum of $|\chi_k^{(k)}(f/f_\alpha)/\chi_k^{(k)}(0)|$ and its trivial counterpart (Fig 1C), which we can ascribe to correlation-induced effects. For $k = 1$ the experimental data agree with the trivial response [convoluted with $\mathcal{G}(\tau)$], consistent with the theoretical arguments stating that glassy correlations do not change the linear response (17). For $k = 3$ and 5 the difference to the trivial response increases, being much more important for $k = 5$ where it exceeds one order of magnitude. This quantitatively supports the scaling prediction obtained assuming that collective effects due to the growth of amorphous order play a key role in supercooled liquids.

We measured $|\chi_5^{(5)}(\omega)|$ at five different temperatures for propylene carbonate (Fig. 2). Propylene carbonate differs from glycerol in that its fragility (27, 28) $m \propto [\partial \log(\tau_\alpha)/\partial(1/T)]_{T_g}$ (T_g denotes the glass transition temperature) is twice as large and it has Van der Waals bonding, in contrast to hydrogen bonding. Despite these differences, the anomalous hump-like features of glycerol (Fig. 1A) are also observed in propylene carbonate (Fig. 2). We expect this behavior from our scaling framework, which relies on the predominant role of collective dynamical effects in supercooled liquids. The presence of similar anomalous features in two very different glass formers suggests they only weakly depend on the specific microscopic properties of the material.

To elicit the temperature dependence of collective effects, we introduced dimensionless quantities related to $\chi_3^{(3)}$ and $\chi_5^{(5)}$:

$$X_3^{(3)} \equiv \frac{k_B T}{\epsilon_0 \Delta \chi_1^2 a^3} \chi_3^{(3)}, \quad X_5^{(5)} \equiv \frac{(k_B T)^2}{\epsilon_0^2 \Delta \chi_1^3 a^6} \chi_5^{(5)} \quad (4)$$

where ϵ_0 is the permittivity of free space, $\Delta \chi_1 = \chi_1(0) - \chi_1(\infty)$ is the dielectric strength, a^3 is the molecular volume and k_B is the Boltzmann constant. The main advantage of these dimensionless non-linear susceptibilities is that in the trivial case of an ideal gas of dipoles, both $X_{3,\text{trivial}}^{(3)}$ and $X_{5,\text{trivial}}^{(5)}$ are independent of temperature when plotted versus scaled frequency (18, 25). Hence, we ascribe their experimental variation to the non-trivial dynamical correlations in the supercooled liquid (17, 23). This interpretation is strongly supported by previous findings (12–14, 23) where the temperature dependence of $|X_3^{(3)}|$ was studied at various values of f/f_α . Close to and above its peak frequency, $|X_3^{(3)}|$ was found to strongly vary in temperature, contrary to the low-frequency plateau region ($f/f_\alpha \leq 0.05$) where $|X_3^{(3)}|$ no longer depends on temperature. This low frequency region corresponds to time scales much longer than τ_α where the liquid flow destroys glassy correlations, making each molecule effectively independent of others, and yielding a dielectric response close to the aforementioned trivial case. This is why, to determine the temperature evolution of the glassy dynamical correlations, we focused on the region of the peak of $|\chi_5^{(5)}|$. For each of the two liquids, this peak appears at the very same frequency f_{peak} as in $|\chi_3^{(3)}|$.

We expect the nonlinear susceptibilities to contain both a trivial contribution that would exist even for independent dipoles, and a “singular” contribution (i.e. diverging with ℓ) as given in Eq. 2. We thus write:

$$X_{3,\text{sing.}}^{(3)} \equiv X_3^{(3)} - X_{3,\text{trivial}}^{(3)}, \quad X_{5,\text{sing.}}^{(5)} \equiv X_5^{(5)} - X_{5,\text{trivial}}^{(5)} \quad (5)$$

Here the trivial contributions are calculated by assuming a set of independent Debye dipoles convoluted with the aforementioned distribution $\mathcal{G}(\tau)$ of relaxation times (18). We compared the temperature evolution of $|X_{5,\text{sing.}}^{(5)}(f_{\text{peak}}(T))|$ and that of $|X_{3,\text{sing.}}^{(3)}(f_{\text{peak}}(T))|^\mu$ (Fig 3), to derive the value of the exponent μ , from which we deduce the fractal dimension d_f of the dynamically correlated regions by using Eq. 3. In both glycerol and propylene carbonate, the value $\mu = 2$, corresponding to compact domains of dimension $d_f = 3$, is found to be consistent with experiments (triangles in Figs 3A and B). By fitting the T dependence of $|X_{3,\text{sing.}}^{(3)}(f_{\text{peak}}(T))|$ with a smooth function (18), we found the hatched area corresponding to $\mu = 2.2 \pm 0.5$ in glycerol and $\mu = 1.7 \pm 0.4$ in propylene carbonate (Fig. 3). The fact that, within experimental uncertainty, a value of $\mu \simeq 2$ is common to each of the two liquids supports a picture of amorphous compact domains mostly independent of differences at the molecular level and validates the correlation length-scale for our scaling analysis. Considering that the temperature interval in Fig. 3B is smaller by a factor of 2, we note that the critical behavior in propylene carbonate is stronger

than in glycerol (Fig. 3A). This suggests that the larger the fragility, the stronger the temperature dependence of the thermodynamic length ℓ . This is easily understood in the scenario of (4) where the critical point is the Vogel-Fulcher temperature T_0 : In this case, equilibrium measurements can be made closer to the critical point for more fragile liquids, because the larger the fragility, the smaller the difference between T_g and T_0 .

Our experimental results are therefore consistent with the general predictions of theories - such as the Random First Order Transition or Frustration Limited Domains (4, 5) - where the physical mechanism driving the glass transition is of thermodynamic origin and where some non trivial (albeit random) long-range correlations build up between molecules. Only in this case (18) can one have N_{corr} dipolar degrees of freedom collectively responding over some length-scale ℓ and on time-scales of the order of τ_α . If instead the glass transition is regarded as a purely dynamical phenomenon, there would not be any anomalous increase of the normalized peak value of the higher-order susceptibilities at all (18). Our results therefore severely challenge theories advocating against any thermodynamic signature and favoring purely dynamic scenarios. Moreover, from a comparison of the higher-order susceptibilities, our results are consistent with $\chi_5 \propto \chi_3^2$. This constitutes evidence for compact amorphously ordered domains, i.e. $d_f = d$, pointing towards a non-standard nature of the glass transition, in contrast to canonical second order phase transitions for which $d_f < d$.

References

1. M. D. Ediger, P. Harowell, Perspective: Supercooled liquids and glasses. *J. Chem. Phys.* **137**, 080901 (2012).
2. L. Berthier, G. Biroli, Theoretical perspective on the glass transition and amorphous materials. *Rev. Mod. Phys.* **83**, 587-645 (2011).
3. D. Chandler, J. P. Garrahan, Dynamics on the way to forming glass: bubbles in space-time. *Annu. Rev. Phys. Chem.* **61**, 191-217 (2010).
4. M. Dzero, J. Schmalian, P. G. Wolynes, in *Structural glasses and supercooled Liquids: theory, experiment, and applications*, P. G. Wolynes, V. Lubchenko, Eds. (Wiley, 2012), pp. 193-222.
5. G. Tarjus, S. A. Kivelson, Z. Nussinov, P. Viot, The frustration-based approach of supercooled liquids and the glass transition: a review and critical assessment. *J. Phys: Cond. Matt.* **17**, R1143-R1182 (2005).
6. S. Mossa, G. Tarjus, Locally preferred structure in simple atomic liquids. *J. Chem. Phys.* **119**, 8069 (2003).
7. G. Biroli, J.-P. Bouchaud, A. Cavagna, T. S. Grigera, P. Verrocchio, Thermodynamic signature of growing amorphous order in glass-forming liquids. *Nature Physics* **4**, 771-775 (2008).
8. R. Pinney, T. B. Liverpool, C. P. Royall, Recasting a model atomistic glassformer as a system of icosahedra. *J. Chem. Phys.* **143**, 244507 (2015).
9. L. Berthier, P. Charbonneau, S. Yaida, Efficient measurement of point-to-set correlations and overlap fluctuations in glass-forming liquids. *J. Chem. Phys.* **144**, 024501 (2016).
10. Y. Kimura, S. Hara, R. Hayakawa, Nonlinear dielectric relaxation spectroscopy of ferroelectric liquid crystals. *Phys. Rev. E* **62**, R5907-R5910 (2000).
11. J.-P. Bouchaud, G. Biroli, On the Adam-Gibbs-Kirkpatrick-Thirumalai-Wolynes scenario for the viscosity increase in glasses. *J. Chem. Phys.* **121**, 7347-7354 (2004).
12. C. Crauste-Thibierge, C. Brun, F. Ladieu, D. L'Hôte, G. Biroli, J.-P. Bouchaud, Evidence of growing spatial correlations at the glass transition from nonlinear response experiments. *Phys. Rev. Lett.* **104**, 165703 (2010).
13. Th. Bauer, P. Lunkenheimer, A. Loidl, Cooperativity and the freezing of molecular motion at the glass transition. *Phys. Rev. Lett.* **111**, 225702 (2013).

14. C. Brun, F. Ladieu, D. L'Hôte, G. Biroli, J.-P. Bouchaud, Evidence of growing spatial correlations during the aging of glassy glycerol. *Phys. Rev. Lett.* **109**, 175702 (2012).
15. U. Buchenau, R. Zorn, M. A. Ramos, Probing cooperative liquid dynamics with the mean square displacement. *Phys. Rev. E* **90**, 042312 (2014).
16. R. Casalini, D. Fragiadakis, C. M. Roland, Dynamic correlation length scales under isochronal conditions. *J. Chem. Phys.* **142**, 064504 (2015).
17. J.-P. Bouchaud, G. Biroli, Nonlinear susceptibility in glassy systems: A probe for cooperative dynamical length scales. *Phys. Rev. B* **72**, 064204 (2005).
18. See supplementary materials on Science Online.
19. L. P. Levy, Critical-dynamics of metallic spin glasses. *Phys. Rev. B* **38**, 4963-4973 (1988).
20. A. Coniglio, A. Fierro, in *Encyclopedia of complexity and systems science*, R. A. Meyers, Ed. (Springer, New York, 2009), pp. 1596-1615.
21. J. D. Stevenson, J. Schmalian, P. G. Wolynes, The shapes of cooperatively rearranging regions in glass-forming liquids. *Nature Physics* **2**, 268-274 (2006).
22. G. Biroli, J.-P. Bouchaud, in *Structural glasses and supercooled liquids: theory, experiment, and applications*, P. G. Wolynes, V. Lubchenko, Eds. (Wiley, 2012), pp. 31-114.
23. F. Ladieu, C. Brun, D. L'Hôte, Nonlinear dielectric susceptibilities in supercooled liquids: A toy model. *Phys. Rev. B* **85**, 184207 (2012).
24. R. Richert, S. Weinstein, Nonlinear dielectric response and thermodynamic heterogeneity in liquids. *Phys. Rev. Lett.* **97**, 095703 (2006).
25. W. T. Coffey, B. V. Paranjape, Dielectric and Kerr effect relaxation in alternating electric fields. *PROC R.I.A.* **78**, 17-25 (1976).
26. T. Blochowicz, C. Tschirwitz, S. Benkhof, E. A. Rössler, Susceptibility functions for slow relaxation processes in supercooled liquids and the search for universal relaxation patterns. *J. Chem. Phys.* **118**, 7544-7555 (2003).
27. P. G. Debenedetti, F. H. Stillinger, Supercooled liquids and the glass transition. *Nature* **410**, 259-267 (2001).
28. R. Böhmer, K. L. Ngai, C. A. Angell, D. J. Plazek, Nonexponential relaxations in strong and fragile glass formers. *J. Chem. Phys.* **99**, 4201-4209 (1993).
29. G. Biroli, J.-P. Bouchaud, K. Miyazaki, D. R. Reichman, Inhomogeneous mode-coupling theory and growing dynamic length in supercooled liquids. *Phys. Rev. Lett.* **97**, 195701 (2006).
30. C. Thibierge, D. L'Hôte, F. Ladieu, R. Tourbot, A method for measuring the nonlinear response in dielectric spectroscopy through third harmonics detection. *Rev. Scient. Instrum.* **79**, 103905 (2008).
31. K. Murata, H. Tanaka, Liquid-liquid transition without macroscopic phase separation in a water-glycerol mixture. *Nat. Mat.* **11**, 436-443 (2012).
32. K. Amann-Winkel, R. Böhmer, F. Fujara, C. Gainaru, B. Geil, T. Loerting, Colloquium: Water's controversial glass transitions. *Rev. Mod. Phys.* **88**, 011002 (2016).
33. D. S. Fisher, D. A. Huse, Ordered phase of short-range Ising spin-glasses. *Phys. Rev. Lett.* **56**, 1601-1604 (1986).

34. M. Baity-Jesi *et al.*, Janus Collaboration, Critical parameters of the three-dimensional Ising spin glass. *Phys. Rev. B* **88**, 224416 (2013).
35. M. Tarzia, G. Biroli, A. Lefévre, J.-P. Bouchaud, Anomalous nonlinear response of glassy liquids: General arguments and a mode-coupling approach. *J. Chem. Phys.* **132**, 054501 (2010).
36. S. Nandi, G. Biroli, G. Tarjus, Spinodals with Disorder: from Avalanches in Random Magnets to Glassy Dynamics. *arXiv:1507.06422*
37. J. C. Dyre, Colloquium: The glass transition and elastic models of glass-forming liquids. *Rev. Mod. Phys.* **78**, 953-972 (2006).
38. A. S. Keys, L. O. Hedges, J. P. Garrahan, S. C. Glotzer, D. Chandler, Excitations are localized and relaxation is hierarchical in glass-forming liquids. *Phys. Rev. X* **1**, 021013 (2011).
39. C. Brun, C. Crauste-Thibierge, F. Ladieu, D. L'Hôte, Third harmonics nonlinear susceptibility in supercooled liquids: A comparison to the box model. *J. Chem. Phys.* **134**, 194507 (2011).
40. The full expression of $\chi_{5,\text{trivial}}$ was provided by P. M. Déjardin (private communication), expanding to the order 5 the calculation published in (41).
41. J. L. Déjardin, Yu. P. Kalmykov, Nonlinear dielectric relaxation of polar molecules in a strong ac electric field: Steady state response. *Phys. Rev. E* **61**, 1211-1217 (2000).
42. C. Brun, F. Ladieu, D. L'Hôte, M. Tarzia, G. Biroli, J.-P. Bouchaud, Nonlinear susceptibilities: Accurate determination of the growing correlation volume in a supercolled liquid. *Phys. Rev. B* **84**, 104204 (2011).

ACKNOWLEDGMENTS

We thank C. Alba-Simionescu, A. Coniglio, P.-M. Déjardin, G. Tarjus, and M. Tarzia for interesting discussions. This work in Saclay has been supported in part by ERC grant NPRGLASS, by the Labex RTRA grant Aricover and by the Institut des Systèmes Complexes ISC-PIF. The work in Augsburg was supported by the Deutsche Forschungsgemeinschaft via Research Unit FOR1394. S.A., R.T., C.W-G. and F.L. developed the Saclay's experimental setup. Th.B. and P.L. developed the experimental setup in Augsburg. Th.B. and M.M. performed the measurements and analysis of the Augsburg data. A.L. and P.L. conceived and supervised the project in Augsburg. G.B. and J.-P.B. derived the theoretical scaling analysis; and all authors were involved in the interpretation of the results and creation of this manuscript. Data are available as supplementary material. All authors have no competing financial interests.

SUPPLEMENTARY MATERIALS

www.sciencemag.org/content/352/6291/1308/suppl/DC1

Materials and Methods

Figs. S1 to S3

References (29–42)

Data files

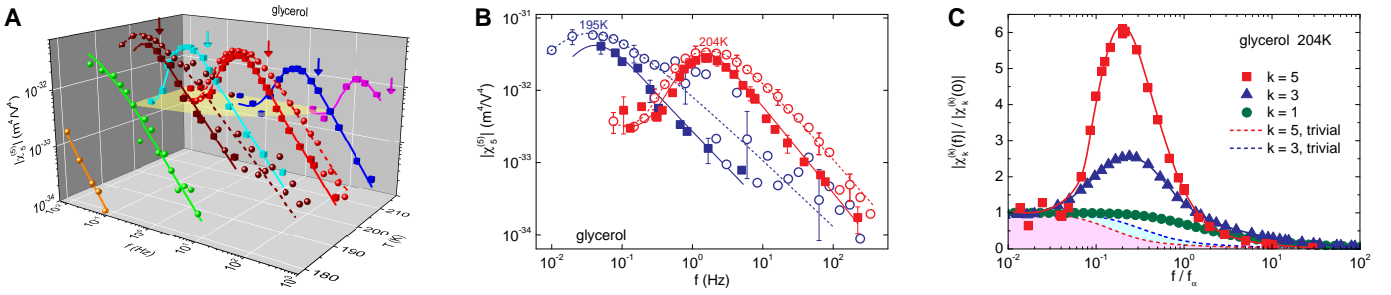


Figure 1: Modulus of the fifth-order susceptibility in supercooled glycerol measured with two independent setups. (A) The susceptibilities $\chi_5^{(5)}$ reported here are obtained directly (18) by monitoring the response of the sample at 5ω , when applying an electric field E at angular frequency ω . Two independent setups were used, designed either to maximize the field amplitude (Augsburg setup, spheres), or to optimize the sensitivity (Saclay setup, cubes). Lines are guides for the eyes. Errors are of the order of the scatter of neighboring data points around the lines. Both setups yield consistent results. For a given temperature T , $|\chi_5^{(5)}|$ has a humped shape, with a maximum occurring at the frequency $f_{\text{peak}} \simeq 0.22f_\alpha$ where f_α is the relaxation frequency indicated by a colored arrow for each temperature. When decreasing T , the height of the hump increases strongly. The yellow plane emphasizes the fact that, for a given T , $\chi_5^{(5)}$ is constant for $f \leq 0.05f_\alpha$. (B) Projection onto the susceptibility-frequency plane of the data of Fig. 1A at 204K and at 195K. The agreement around and below the peak is remarkable at 204K (see text). The relative evolution of the height of the peak is reasonably similar between 204K and 195K for the two setups (see Fig. 3A). (C) Comparison of the fifth-order, cubic, and linear susceptibilities of glycerol [the latter is noticed $\chi_1^{(1)}$ for convenience, see (18)]. Symbols, with line to guide the eyes, are Saclay data at 204K; the error bars are of the order of the size of the symbols for $k = 5$ [except at the lowest frequencies, see (18)] and smaller for $k = 3$ and 1. The higher the order k , the stronger the hump of $|\chi_k^{(k)}|$: this is a key result supporting the amorphous-order scenario. The dashed lines, emphasized by colored areas, correspond to the trivial response of an ideal gas of dipoles without amorphous order. In this case $|\chi_k^{(k)}|$ decreases monotonously in frequency for any value of k . The higher k , the stronger the difference between the measured and trivial susceptibility.

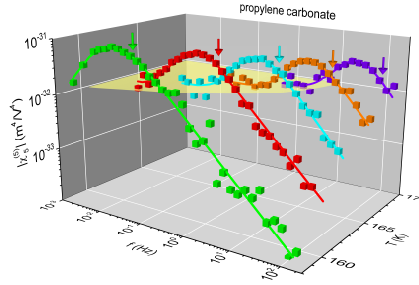


Figure 2: **Modulus of the fifth-order susceptibility in supercooled propylene carbonate.** The experimental data (symbols) were obtained with the Augsburg setup. The presentation of the graph is analogous to that of Fig 1A to emphasize the similarity of the behavior of $|\chi_5^{(5)}|$ in propylene carbonate and in glycerol, even though these two liquids have different fragilities and different types of intermolecular interactions (van der Waals versus hydrogen bonding).

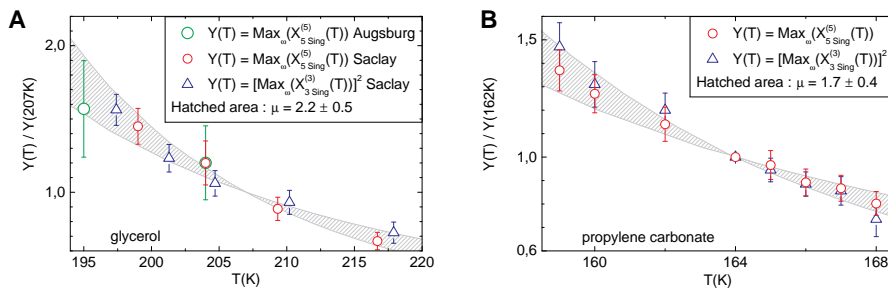


Figure 3: **Comparison of the temperature dependence of the singular part of the fifth order and cubic dimensionless susceptibilities at f_{peak} .** (A) For glycerol, the singular part of $|X_k^{(k)}(f_{\text{peak}})|$ for $k = 3$ and 5 is normalized to 1 at 207K. The value of the exponent μ is then determined by comparing $|X_5^{(5)}(f_{\text{peak}})|$ to $|X_3^{(3)}(f_{\text{peak}})|^\mu$: the symbols for $k = 3$ correspond to $\mu = 2$ and the hatched area to the interval corresponding to the error bar given for μ (18). The two Augsburg data points for $X_5^{(5)}$ have been added on the graph by scaling to the Saclay point at 204K: the Augsburg point at 195K is reasonably well within the hatched area, which shows that the relative evolution of $X_5^{(5)}$ with temperature is consistent in the two setups. (B) Same display as in (A) but for propylene carbonate with $T = 164\text{K}$ as the normalization temperature and the symbols for $k = 3$ corresponding to $\mu = 2$.